Emergent Materials (2025) 8:7463–7480
https://doi.org/10.1007/s42247-025-01175-9

ORIGINAL ARTICLE

Predicting Common Rail Direct Injection (CRDI) engine metrics using nanoparticle-enhanced pongamia pinnata biodiesel with machine learning

Joga Rao Bikkavolu[1] · Rakesh Kumar Tota[2] · Ravi H[3] · Kodanda Ramarao Chebattina[4] · Lakshmipathi Raju Bhagavatula[4] · Gandhi Pullagura[4] · PraveenKumar Seepana[5]

Received: 25 April 2025 / Accepted: 19 June 2025 / Published online: 23 July 2025

Abstract

The effective use of fossil fuels in compression ignition (CI) engines results in hazardous pollution into the atmosphere. Many scholars explored using biodiesel and its blends to replace fossil fuels and reducing hazardous emissions. The current study extends preparation of biodiesel through transesterification process from the karanja oil feed stock as an alternative energy for twin cylinder, Common Rail Direct Injection (CRDI), CI engines. Moreover, various types of metal and non-metal-based nanoparticles (NPs) are dispersed in karanja oil based B20 (20% of biodiesel is blended in 80% of diesel) sample in the presence of QPAN80 surfactant. To prepare stable and homogeneous nano assisted fuel blends the optimum ratio of 1:4 (NPs to surfactant) is used. The Diesel R-F Simulation software is used to find the calibration of CI engine using diesel fuel. The cylinder pressure (CP), brake thermal efficiency (BTE) are found to be 5% variation, while the brake specific fuel consumption (BSFC) is with in the 10% range. The performance parameters are found to be enhanced BTE increased by 9.8%, and BSFC is decreased by 18.7% for B20CNT50 mix at maximum brake power (BP) as compared to B20 blend. Further, the emission characteristics including carbon monoxide (CO), carbon dioxide (CO_2), hydrocarbon (HC), and smoke are found to decrease by 7.71, 11.2, 10.2, and 5.71% for B20CNT50 mix at higher BP as correlated to D100 sample. Nevertheless, the nitrogen oxides (NOx) emission is lowered by 10.9% for B20CNT50 blend than the B20 mix at maximum BP. These findings disclosed that the B20CNT50 sample offers higher performance and lower emission characteristics and potential to use in CRDI, CI engines without engine modifications. Additionally, machine learning algorithms such as support vector regression (SVR), and random forest (RF) are implemented in accurately predicting engine performance and emission characteristics by analyzing relationships between input and output parameters. Their ability to model these interactions enables optimized engine design and reduced experimental cost.

Keywords Karanja oil · Diesel R-F simulation software · CRDI · Emissions · Nanoparticles · ML methods

✉ Gandhi Pullagura
gpullagu@gitam.edu

[1] Department of Mechanical Engineering, Godavari Global University, Rajahmundry 533296, India

[2] School of Marine Engineering and Technology, Indian Maritime University, Chennai 600119, India

[3] Department of Mechanical Engineering, GITAM (Deemed to be University), School of Technology, Hyderabad 502329, India

[4] Department of Mechanical Engineering, GITAM (Deemed to be University), School of Technology, Visakhapatnam 530045, India

[5] Department of Nuclear and Renewable Energy, Ural Federal University Named After the First President of Russia Boris Yeltsin, 19 Mira Street, Ekaterinburg 620002, Russia

1 Introduction

The excellent capabilities of a CI engines in terms of load carrying abilities, greater BTE and better fuel economy which is mainly due to self-governing ability have made it to use in different fields including automotive industry, marine, power generation, transportation etc [1, 2]. On other side, the continues utilization of diesel fuel from fossil based resources causing to increase demand enhancing the oil prices [3, 4]. Moreover, the fossil based fuels emit hazardous pollution such as CO, NOx, and HC which distracts the environmental ecosystem and humans health (Causing respiratory issues, heart attacks, asthma, absenteeism).

Based on the reports of World Health Organization (WHO), around 3 million people are dying annually from the environmental deterioration [5]. Nevertheless, the need and demand of power requirements urge to use fossil based fuels which will deteriorate in a decade [6].

This challenging situation forces researchers to search for alternative energy sources. In this scenario, biodiesel research has received significant attention despite of its numerous advantages such as improved combustion efficiency, lower engine exhaust emissions, and an environmentally benign fuel source. It is evidenced from the previous literature that the biodiesel is biodegradable, non-toxic, and renewable has made it a dependable replacement for diesel fuel [7, 8]. Transesterification process is commonly employed to turn into biodiesel which helps to reduce the viscosity of the raw oils derived from edible/non-edible feed stock and improve the physio-chemical properties of the biodiesel [9]. Non-edible feedstocks are the best suited to provide maximum biodiesel yield, easy availability, use waste land, consume less water, minimize the competency of human food resources, and less feedstock cost. In the present study, biodiesel is prepared from karanja oil feed stock due to availability, Its rich oil content (30–40%), and high calorific value (35.9 MJ/kg). The scientific name of karanja tree is *pongamia pinnata* which can grow widely in tropical conditions like rural places in India, Assam, western Ghats and also most commonly available in China, Africa, Japan, and Australia [4, 10]. It possess free fatty acid content of linoleic acid (10.8–18.3%), stearic acid (2.4-9%), and oleic acid of (44.4–71.3%), palmitic (3.7–7.9%), behenic (4.2–5.3%), arachidic (2.2–4.7%) and lignoceric (1.1–3.5%) [11, 12]. Besides, biodiesel cannot be fueled in CI engines due to their poor cold filter plugging point, cold flow properties in low temperature, poor energy content, higher viscosity, and greater NOx emissions. It can, however, be blended up to 20% vol in 80% vol of pure diesel fuel to create a B20 mixture, which is a most widely approved fuel mix proportion for testing on diesel engines with no engine modifications [1].

Though the B20 sample proves to be the supplementary fuel to the conventional diesel engines, many researchers showed limitations in overall engine performance due to lower heating value of the B20 mix, higher viscosity, low oxidation stability, and higher fuel consumption. Moreover, the hazardous NOx emission is generated which is owing to comprehensive combustion, and greater engine cylinder temperature that results in NOx emissions. In this aspect, researchers focused on NPs dispersion and oxygenated additives to improve the physio-chemical properties of the samples which facilitates to enhance the performance and reduce the emissions of CI engine [13]. Researchers employed different fuel reformulation techniques in which dispersion of various metal/metal oxide NPs are very common since their ability to enhance the performance, and decrease the pollutants [14, 15]. The NPs posses greater surface to volume ratio, improved catalytic activity, greater thermal conductivity which facilitates to enhance the fuel blend's physiochemical characteristics and boost the overall performance, and minimize the pollutants. For an instance, Nutakki et al. [16] stated that the dispersion of silicon oxide (SiO_2) NPs (at a quantity of 40, 80, and 120 ppm) in mahua oil based B20 sample performed better on CRDI, CI engine over diesel fuel. The results declared that the BTE is marginally improved and BSFC is reduced. While, CO, HC, and smoke emissions are lowered but, NOx emissions showed slightly increased trend. In a research work carried out by Srinivasan et al. [17] that the dispersion of titanium oxide (TiO_2), and alumina (A) NPs at a quantity of 25, and 50 ppm in rubber seed oil based B100 employed in CI engine as an alternative fuel. The outcomes of the study showed that the performance characteristics are increased (BTE is raised by 5.2% and BSFC is lowered by 10.56%). while, emission characteristics are found to be decreased (HC, CO, and Smoke by 28, 44, and 44%) except NOx (improved by 21%) as correlated to diesel at higher load. Surendra Babu et al. [18] explored that the dispersion of copper oxide (CuO) NPs (at a quantity of 50, and 100 mg/l) blended in pumpkin seed oil based B20. The findings disclosed that the BTE is enhanced by 2.3% while BSFC is decreased by 6.4%. Further, the pollutants such as CO, HC, and smoke are decreased. On other side, the NOx emissions are found to improve marginally. Further, the combustion parameters such as Heat Release Rate (HRR), CP are improved for B20 included CuO NPs at a dosage of 100 ppm and at maximum load. In another article Prabhu [19] stated that the inclusion of A NPs at a quantity of 100 ppm in waste transformer biodiesel diesel blends results in enhanced BTE by 6% at higher injection timing as compared to diesel. While, HC, CO, and smoke are decreased by 33, 8, and 1.5%. Moreover, the NOx emissions are improved by 9.7%.

The use of metal/metal oxide NPs showed deficient in exhaust gas emission reduction majorly NOx and Because of their tiny stature and unique characteristics, NPs can be harmful to human health and cause several various health issues [20]. In recent years, scholars employing non-metal carbon based NPs in fuel blends which inhibits releasing hazardous components. These NPs posses greater surface to volume ratio, greater thermal properties, and improves rate of reaction. The NPs act as secondary energy carrier and improves heat transfer rate which reduces ignition delay (ID) and enhances combustion and reducing emissions. In an investigation concluded by Nair et al. [21] that the addition of graphene nanoplatelets (GNPs) at a dosage of 25, 50, and 75 mg/l in karanja based B20 sample showed in

enhanced performance parameters and emissions including CO, HC, and NOx are particularly lowered for B20G75 sample at higher load. In another article authored by Arumugam & Muralidharan [22] showed that the addition of non-metallic oxides such as graphene oxide (GO) NPs in geranium oil based B20 increased performance parameters (BTE by 5.92% and decreased BSFC by15.5%). Moreover, the combustion properties such as CP and HRR are enhanced which is owing catalytic effect of NPs and thus, resulting in reduced ID. In a research article investigated by Pullagura et al. [23] experimented that the GNPs NPs at a dosage of 25–75 mg/l at a range of 25 dispersed in sterculia foetida based B20 sample on a CI engine. The findings proved that the addition of GNPs at a dosage of 50 mg/l results in increasing BTE by 8.48% and BSFC, CO, HC, and NOx were observed to be decreased by 16.53, 24.1, 28.3, and 10.43% respectively at higher loads. Nevertheless it was also stated that the combustion parameters such as ID, and combustion duration (CD) are diminished while, CP, and HRR are increased which is attributed to better thermal conductivity, improved rate of reaction, and greater surface to volume ratio of NPs. In another experimental investigation carried out by Bikkavolu et al. [5] studied that the effect of carbon nanotubes (CNTs) at a concentration of 25, 50, and 75 mg/l in yellow oleander based B20 sample on a single cylinder, diesel engine. It is observed from the study that the inclusion of CNTs in B20 showed that the dispersion is more stable in the base fuel suspension and improved physio-chemical properties. Further, the blend containing 50 mg/l of CNTs in B20 sample enhanced BTE by 15.5% due to improved air-fuel mixing, and catalytic activity of NPs. Moreover, the BSFC is reduced by 20.57% and emissions parameters such as CO, HC, and NOx are decreased by 26.8, 35.7, and 13.2% respectively at maximum brake power condition which is due to oxygen buffer in the cylinder, and improved rate of reaction. Nevertheless, the improved combustion properties such as CP, and HRR are enhanced, and ID, and CD are lowered. In a similar study, Sulochana et al. [24] explored that the addition of multi - walled carbon nanotubes (MWCNTs) at a dosage of 25, and 50 mg/l in B20 sample and fueled to evaluate the performance, and emission parameters on a CI engine. The test results disclosed that the addition of 50 mg/l MWCNTs in B20 fuel mix resulted in improved BTE by 25%, and decreased BSFC by 17%. This enhancement is due to proper air fuel mixing, improved fuel evaporation and atomization, and influence of NPs. While, NOx pollution is decreased by 36% which is due to reduced cylinder temperature, and heat absorption capacity of NPs. In another investigation explored by Soundararajan et al. [25] stated that the inclusion of graphene quantum dot (GDQ) NPs at a dosage of 30, 40, and 50 mg/l in waste plastic oil based B20 to evaluate the engine overall performance, and emission parameters. The outcomes indicated that the addition of 40 ppm NPs in B20 sample resulted in enhanced BTE by 5.71% while, emission parameters NOx, and smoke are decreased by 1.63, 2.33 respectively. On other side, the significant combustion also showed decreased CO, and HC pollutants.

Recent advancements in predictive modeling and optimization techniques for internal combustion (IC) and dual-fuel engines have prominently featured machine learning (ML) approaches, to forecast performance and emission characteristics. While traditional statistical models offer valuable insights, they often assume linearity and require predefined functional relationships between variables, which may not accurately capture the complex, nonlinear behavior of engine performance and emissions influenced by biodiesel blends and nanotechnology. In contrast, machine learning algorithms are capable of modeling intricate, high-dimensional interactions without requiring explicit assumptions about data distribution. Given the multi-factorial nature of combustion processes and the synergistic effects of fuel composition and nano additives, ML methods provide a more flexible and data-driven approach for achieving high predictive accuracy and uncovering hidden patterns, making them especially suitable for this study. Recent works have demonstrated the capability of machine learning models to effectively predict key engine parameters such as BTE, BSFC, and emissions including CO, HC, and NOx. Artificial neural networks (ANN) have been widely used for this purpose. For instance, Varma et al. [26] reported that an ANN model applied to a CRDI engine running on biodiesel blends achieved a high correlation coefficient of 0.99742 in predicting BTE and NOx emissions, indicating excellent model accuracy. Similarly, SVM have also been employed, with Liao et al. [27] highlighting their superior predictive performance over ANN. Their study reported maximum prediction errors of less than 5% in emission parameters and demonstrated SVM's effectiveness in optimizing injection strategies to reduce NOx and soot formation. In addition to machine learning, the incorporation of nanoparticles as additives in biodiesel blends has been found to significantly influence engine performance and emissions. Cerium oxide (CeO_2) nanoparticles, for example, have shown potential in improving combustion characteristics while simultaneously reducing CO and HC emissions [28]. Similarly, zinc oxide (ZnO) nanoparticles have been reported to enhance brake thermal efficiency, reduce BSFC, and improve brake power [29]. While machine learning models such as ANN and SVM provide robust frameworks for predicting performance and emissions, their efficacy is inherently dependent on the quality and volume of training data. Insufficient or noisy datasets may lead to over fitting and limit the generalizability of the model under varying operating conditions. Hence, coupling

high-fidelity experimental data with advanced ML models is crucial to achieving reliable and scalable predictive solutions for CRDI engines fueled with nano enriched biodiesel blends. A study employing a gaussian process regression - feedback neural network algorithm (GPR-FNN) [30] model demonstrated high accuracy in predicting BTE, BSFC, and emissions including carbon Monoxide CO, HC, and NOx in dual-fuel engines. Another investigation [31] focused on BTE, BSEC, and exhaust emissions (CO, HC, and NOx) using an ANN based approach. The results examined the effectiveness of neural networks in capturing complex, non-linear engine behaviors under dual-fuel combustion conditions. The reviewed literature [32] reveals a growing trend toward ML-based engine performance modeling. While several studies demonstrate the power and accuracy of ML and hybrid models in predicting engine outputs and emissions, notable gaps remain in the integration of all critical parameters within a singular comprehensive framework. This underscores the need for future research to adopt more holistic approaches, incorporating both ML techniques and extensive performance-emission interrelations. In this work, ML methods are implemented to address the prediction capabilities of engine performance and emission characteristic curves.

1.1 Present work and novelty

From the above literature study, the various types of NPs dispersed in the biodiesel diesel blends. But, the metallic, and non-metallic NPs are not employed in any non-edible oil-based biodiesel-diesel blends to test on CI engine. Hence, the current study aims to explore the influence of metallic, and non-metallic NPs in karanja oil based B20 sample to evaluate the performance, and emission parameters under different Loads. Initially, the diesel engine is tested with diesel fuel and compared with the diesel R-F simulation software to find the comparison and validation. Then the prepared fuel samples are experimented on the validated CI engine to analyze the performance, and emission characteristics. This research is intended to find the feasible and sustainable energy source for CI engines with no engine modifications employing nonmetallic NPs assisted karanja oil based B20 sample.

The investigation has the objectives below:

- To determine the best biodiesel yield through the transesterification process.
- To evaluate the performance, and cylinder pressure of a CI engine using diesel fuel and compare with the experimentation and simulation for validation.
- To investigate the performance, and emission parameters of a CI engine using karanja oil based Biodiesel-diesel blend with different NPs.
- To provide recommendations and possible research directions for improving and commercializing the karanja oil biodiesel-diesel blends with NPs addition in diesel engines in order to achieve improved performance, reduced emissions, and sustainable energy sources.

2 Materials and methodology

2.1 Biodiesel preparation

Karanja oil was obtained from the local market in Visakhapatnam, India. The oil is heated to boiling point of water 100°C to eliminate the moisture. The free fatty acids (FFA) of the purified oil is found to be Palmitic, Oleic, and Linoleic [11, 12]. The acid and base catalyst are used to prepare methyl ester due to greater acidity in the oil. The oil was initially heated to 70°C and then, blended with 100 g of methanol and Sodium hydroxide (NaOH) in a round flask and mixed vigorously using magnetic stirrer for homogeneous blend. After the reaction, the treated solution is transferred into separating funnel. Then, the glycerol, residual methanol, unreacted catalyst, and moisture were eliminated from the funnel after washing with worm water and heating to 100°C. The highest karanja oil methyl ester (KOME) yield obtained was 97.8% employing the below Eq. 1. Figure 1a. shows the steps involved in KOME preparation [12].

$$Biodiesel\ yield\ (wt\,\%) = \left[\frac{mass\ of\ biodiesel\ (g)}{mass\ of\ oil\ (g)}\right] x\ 100 \quad (1)$$

2.2 Surface modification of nanoparticles and Preparation of fuel samples

The NPs dispersed in the base fluids must be stable and uniform to accomplish the superior properties. In this aspect, the dispersants called surfactants are coated on NPs (A) at different ratios (NPs to surfactants (QPAN80)) such as 1:1, 1:2, 1:3, 1:4, and 1:5 in the presence of hexane sample using water bath and probe sonicator (Hielscher ultrasonic, 160 W, 40 kHz) for 30 min to eliminate agglomeration, and sedimentation. Then, the blended solution is allowed to dry for 24 h. After drying, the surface coated NPs are mixed in 20% vol. of KOME-80% vol. of diesel blend (B20) at a fixed quantity (50 mg/l) employing bath and probe sonicator for 10 min each. Out of these five trails, the optimum ratio of 1:4 shown positive impact on stability and homogeneity and is set as benchmark. The same ratio is used for surface modification and a quantity of 50 mg/l surface modified

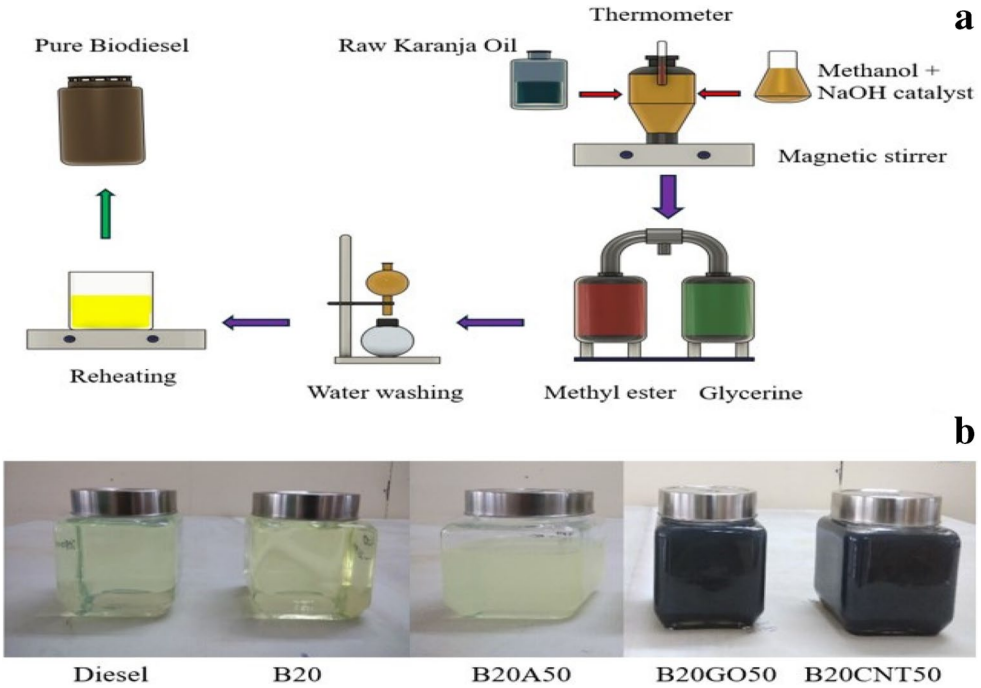

Fig. 1 **a** Illustration of the preparation of biodiesel using karanja seed oil. **b** Diesel, and B20 blends with different nanoparticles

Table 1 Physico-chemical properties of fuel samples with and without addition of NPs

Properties	Method	Test limit ASTM D6751-15c	Diesel	B2O	B20A50	B20GO50	B20CNT50
Density @15 °C	ASTM D-4052	815–840	833.1	837.9	838.0	837.1	836.4
Calorific value/(MJ/kg)	ASTM D-224	Min. 35,000	42,600	40,759	40,871	41,130	40,970
Kinematic viscosity, cSt, @40 °C	ASTM D-445	1.8–4.2	2.59	3.8	3.44	3.4	3.37
Copper strip corrosion	ASTM D130	Max. 3	1	1	-	-	-
Cetane number	ASTM D-13	Min. 40	44.45	49	53.8	54.49	53.85

Table 2 Specifications of nano particles

Al_2O_3	GO	CNTs	Item
Platonic Nanotech Private Limited-Kachwa Chowk, Dist: Godda, Jharkhand			Supplier
Aluminum oxide	Graphene oxide	Carbon nano tubes	Name of the chemical
11.4 W/m k,	670 W/(m K)	3,000 watts/m-k	Thermal conductivity
White	Black	Black	Color
74 m^2/g	200 m^2/g	200–240 m^2/g	Surface area (SSA)
20 ± 5 nm	1 to 4 nm	5–10 nm thickness, length 5 micron	Average particle size

NPs (GO, CNTs) are blended in B20 [12]. The prepared fuel blends are termed as B20A50, B20GO50, and B20CNT50. The prepared blends are found to be homogeneous, which is evidenced by characterization. The prepared samples including B20, B20A50, B20GO50, and B20CNT50 are shown in Fig. 1b. and these samples are used to evaluate physio-chemical characteristics shown in Table 1.

2.3 Characterization

The NPs such as aluminum oxide (Al_2O_3), GO, CNTs are supplied by platonic nanotech private limited jharkhand; Table 2. Provides comprehensive specifications. According to Cao et al., [33] field emission scanning electron microscopy (FESEM) allows for direct evaluation of NPs alignment and size details. The morphology of NPs was examined using FESEM (Model: Quanta FEG250) at the MURTI facility GITAM Deemed to be University-Visakhapatnam. High-resolution transmission electron microscopy (HRTEM) study (JEOL; JEM 2100 F, FEG TEM 200 kV) were utilized.

The surface and morphological characterization of NPs was performed using FESEM and HRTEM. The findings obtained for each NP are displayed in Fig. 2. FESEM pictures were generated at 120,000X magnification. Figure 2 shows that Al_2O_3 NPs were spherical and smooth-surfaced, with an average particle size of 30 nm, indicating that the NPs were smaller in size than the fuel injector's nozzle diameter without blocking fuel flow in the nozzle. Figure 2 showed a resolution of 200 nm and a magnification of

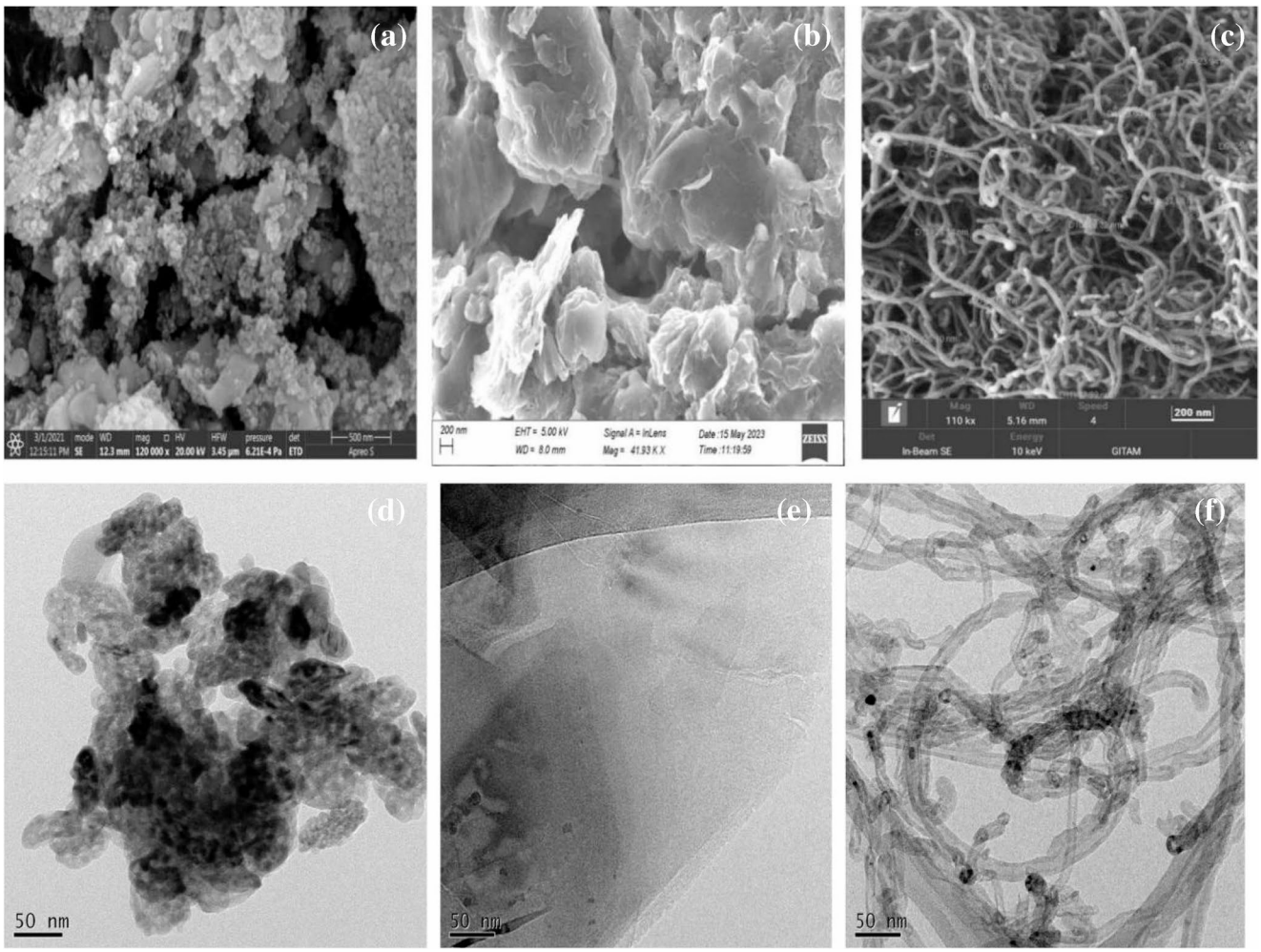

Fig. 2 Depicts the FESEM & HRTEM images of Al_2O_3, GO, and CNTs

41.93 KX. GO NPs exhibit remarkable mechanical characteristics, good electrical conductivity, great charge carrier mobilities, high TC, specific magnetism, large surface areas, and exceptional electro-catalytic activities [12]. Because of their distinct characteristics, GO NPs are an important contribution to improving fuel properties. The FESEM picture of CNT Fig. 2(c) shows that the nanotubes had an average diameter of 20–25 nm and a length of 5–15 µm. CNTs are a useful additive for enhancing fuel characteristics.

The Fourier transform infrared spectroscopy (FTIR) is used to determine the bonds and functional groups in Al_2O_3, GO, and CNT. Figure 3. Depicts the transmissivity values between 500 cm^{-1} and 4000 cm^{-1}. Figure 3(a) indicates that peaks at 3600–2500 cm^{-1} correspond to γ-Al_2O_3 with varying -OH groups on the exterior. The peaks below 920.67 cm^{-1} were associated with Al-O vibrations. A sharp band at 1410.46 cm^{-1} indicates scissoring vibrations of two O-H bonds in physically absorbed water molecules or a small amount of adsorbed pollutants, such as CO_2 or carbonates [34]. In Fig. 3(b), the troughs at 917.16 cm^{-1} indicate the presence of C-O. Absorbance dips at 2916.35 cm^{-1} indicate the existence of hydroxyl groups. Figure 3(c) reveals that the absorption dips at 1462.4 cm^{-1} and 2914.23 cm^{-1}, indicating the existence of C-OH and hydroxyl groups.

2.4 Experimental setup

In the present investigation, a twin-cylinder, four-stroke, water cooled, CRDI, diesel engine is used as shown in Fig. 4(a). A fuel tank, fuel pipe, and air box are attached to the engine. Water flow rate is measured by a rotameter while, flow transmitters are used to measure the fuel and air. The exhaust system is equipped with a calorimeter to reduce the exhaust gas temperature. Other devices such as temperature sensor, pressure sensor, in-cylinder pressure transducers, eddy current dynamometer, and engine load sensor are used along with the diesel engine for data collection during the experiment for 100 cycles. The nano assisted fuel samples and B20 are tested on the CRDI, diesel engine. These tests are conducted under atmosphere conditions and each test is

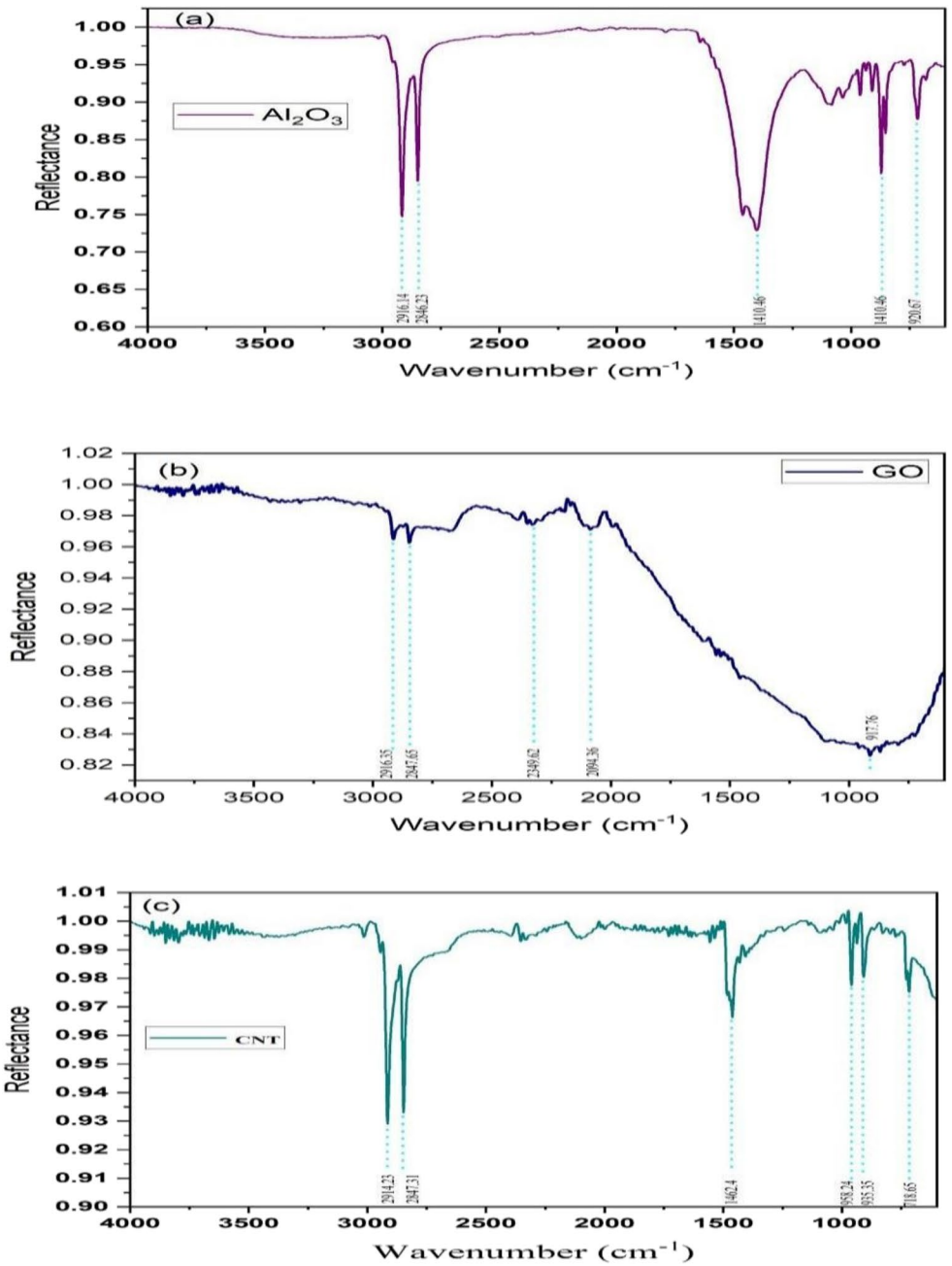

Fig. 3 FTIR Analysis of (**a**) Al_2O_3, (**b**) GO, and (**c**) CNT nanoparticles

conducted for five times to achieve repeatability reproducibility and replicability. The technical details of the engine set up are given in Table 3. Figure 4b depicts the engine arrangement details.

2.4.1 Uncertainties in experimentation

The selection of testing equipment is the initial step that causes errors and uncertainties in measurements [35]. The experiments' accuracy is proven using uncertainty analysis [36]. The errors in the results are due to an imperfection in the parameter measurement. The percentage uncertainties of the instruments employed in the experimental section to modify engine load and assess engine findings were estimated using the error propagation theory, as shown in Table 4. The uncertainty found during the experimental phase of the study for comparing experimental and numerical findings is assumed to exist for testing with all fuel samples. As a result, the error graphs reflecting uncertainty were incorporated into the numerical simulation results. The overall uncertainty is given in Eq. 2 and it is found to be 2.46%.

The below equation evaluates the overall uncertainty:

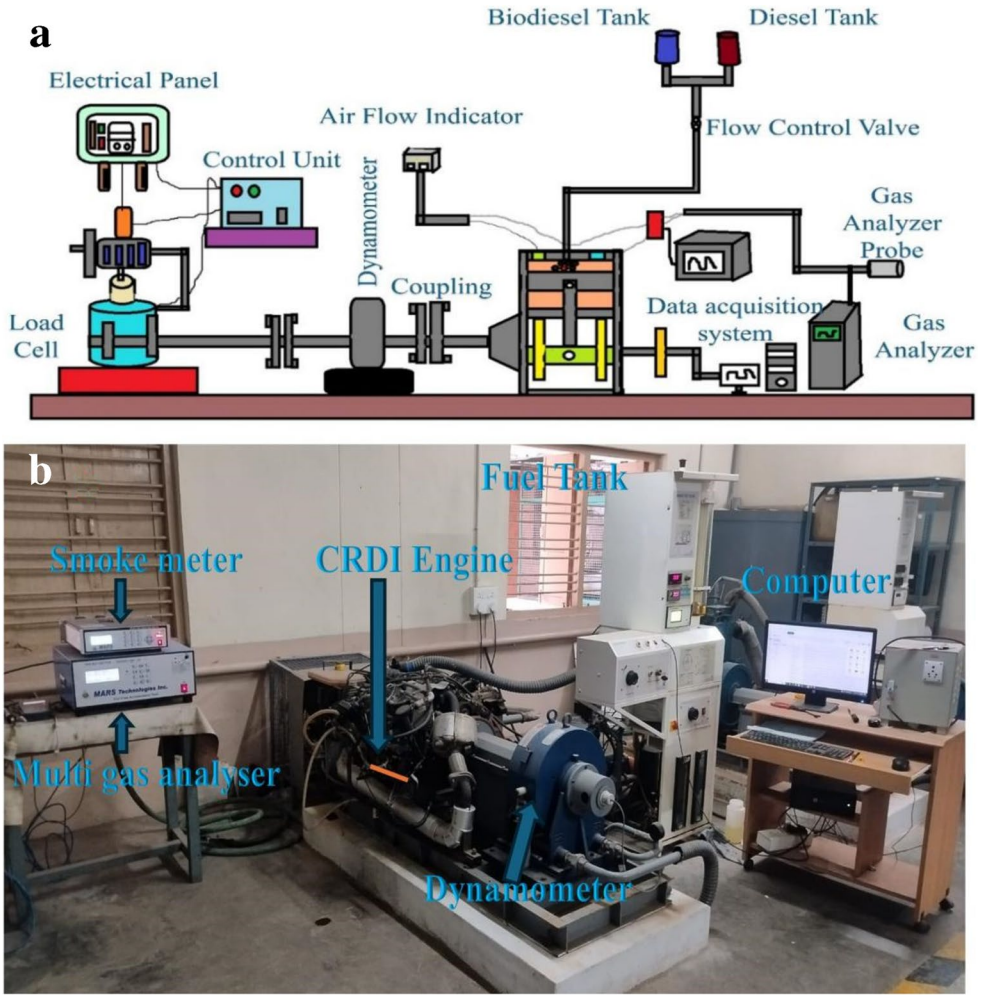

Fig. 4 Illustrates the details of engine arrangement

Table 3 Technical specifications of testing engine

Particulars	Description
Engine type	2-Cylinder, 4-stroke, CRDI,
Engine rated power	35 kW
Cylinder dia and Stroke length	83 mm and 84 mm
Cooling type	Water cooled
Injection pressure	500 Bar
Injection timing	23° before TDC
Orifice diameter	35 mm
Dynamometer arm length	210 mm
Compression ratio	18.5: 1
Inlet valve opening and closing	4.5° before TDC and 35.5° after BDC
Outlet valve opening and closing	35.5° before BDC and 4.5° after TDC

$$= \sqrt{u_{(BTE)}{}^2 + (u_{BSFC})^2 + (u_{CO})^2 + (u_{HC})^2 + (u_{NOx})^2 + (u_{CO2})^2 + (u_{Smoke})^2} = \sqrt{(0.75)^2 + (0.25)^2 + (1)^2 + (1)^2 + (1)^2 + (1.2)^2 + (1)^2 + (1)^2} = \pm\ 2.46\% \quad (2)$$

where:

u_{BTE} Uncertainty of Brake Thermal Efficiency.
u_{BSFC} Uncertainty of Specific fuel consumption.
u_{CO} Uncertainty of CO emission.

Table 4 Uncertainty of measurement

Measurement	Accuracy	Uncertainty (%)
Temperature sensor	±1.5 °C	±0.20
Piezoelectric pressure sensor	±0.20 bar	±0.10
Eddy current dynamometer	±0.02%	±0.20
PNP Speed sensor	±10 rpm	±1.00
Crank angle encoder	±0.10 CA bTDC	±0.10
Optical burette fitted measurement	±0.20%	±0.20
Strain gauge load cell sensor	±0.02%	±0.15
AVL Gas analyzer	±0.10%	±1.00

u_{HC} Uncertainty of HC emission.
u_{NOx} Uncertainty of NOx emission.
u_{CO2} Uncertainty of CO_2 emission.
u_{smoke} Uncertainty of Smoke.

2.5 Machine learning analysis

The goal of machine learning analysis in the present work is to predict multiple output variables such as BSFC, BTE, CO,

CO_2, HC, NOx, and smoke opacity based on input variables like brake power, speed, and compression ratio. These output variables are critical in evaluating engine performance and emissions, and they have a strong relationship with the input features. The machine learning approach should use Regression techniques are used in the ML approach as these outputs are continuous numerical values. The model will be trained on a pre-processed dataset with clean and normalized data to ensure the features are scaled appropriately for model performance. The model will then learn from the data to identify patterns that relate input features to the outputs, with the aim of making accurate predictions. The process begins with data import and loading, where essential Python libraries such as Pandas, NumPy, Seaborn, Matplotlib are imported. The dataset is then loaded with Excel files. Next is data pre-processing, which includes normalization, input features such as brake power, speed, and compression ratio are scaled to similar ranges using techniques like Min-Max scaling or Z-score normalization.

For ML model selection, an appropriate regression model is chosen based on the complexity of the relationship between input and output variables. In present work, SVR and RF algorithms were employed to predict engine performance and emission characteristics based on experimental data. For the SVR model, a radial basis function (RBF) kernel was selected due to its effectiveness in capturing nonlinear relationships. Hyper parameters were optimized using a grid search approach, with the regularization parameter C ranging from 1 to 100 and the kernel coefficient ϒ ranging from 0.01 to 0.1. The RF model was configured with 100 decision trees and a maximum depth tuned between 10 and 30 to prevent over fitting while maintaining model accuracy. To ensure robust model training and evaluation, the data set was randomly divided into 80% for training and 20% for testing, with 5-fold cross-validation applied during training for hyper parameter tuning and validation. Model performance was assessed not only using accuracy but also through a comprehensive set of metrics, including the coefficient of determination (R^2), mean absolute error (MAE), mean square error (MSE) as mentioned in Eqs. (3–5). These metrics provided a more reliable and multidimensional evaluation of each model's predictive capability in estimating output variables such as Brake Thermal Efficiency BTE, BSFC, and major exhaust emissions (CO, HC, and NOx). Actual vs. predicted values are compared visually using scatter plots or residual plots to identify any patterns or errors. Finally, in the model deployment phase, the trained and validated model is deployed to generate predictions on new, unseen data, making it ready for predicting the output variables. The step by step work flow of the procedure is shown in Fig. 5.

$$\text{Coefficient of Determination}: \ \mathrm{R}^2 = 1 - \frac{\sum_{i=1}^{n}(\widehat{y}_i - y_i)^2}{\sum_{i=1}^{n}(\overline{y}_i - y_i)^2} \tag{3}$$

$$Mean\ square\ error: \ \mathrm{RMSE} = \frac{1}{n}\sum_{i=1}^{n}(\widehat{y}_i - y_i)^2 \tag{4}$$

$$Mean\ absolute\ error: \ \mathrm{MAE} = \frac{1}{n}\sum_{i=1}^{n}|\widehat{y}_i - y_i|. \tag{5}$$

where n represents the number of test samples, y_i experimental result value, $\widehat{y}_i$ predicted output value from the ML model, and $\overline{y}_i$ represents the mean of the experimental result values.

3 Results and discussions

3.1 Experimentation and validation

A standard diesel engine is used to test the neat diesel in the current study. The CI engine is fueled with diesel and runs at different load conditions. During the test, parameters such as torque, BP, fuel consumption, and exhaust emissions are recorded using Diesel R-K simulation software with the appropriate engine data. The results from the software are compared with the experimental data for validation. The software predicts the engine overall performance, and emission parameters employing significant thermodynamic relations to Diesel R-K equations as given in Table 5. Figure 6 explains the comparison between experimental and numerically predicted data for 6 (a) Cylinder Pressure vs. Crank Angle, and 6 (b) BTE and BSFC vs. Brake Power based on Diesel R-K simulation software for validation process [37]. The peak CP, BTE, and BSFC are observed to be 76.16 bars, 32.7%, and 0.262 kg/kWh experimentally while, the same parameters are found to be 78.62 bars, 33.7%, and 0.237 kg/kWh numerically. The experimental and numerical values are well correlated and proportional to each other and BTE, and CP are found to be within the variation of 5% while BSFC values are in the variation of 10%. The close relationship between actual and simulated findings confirms the validity of the experimental setup and measurement procedures. The experimental study is continued for obtaining the performance, combustion, and emission parameters for the remaining fuel blends including D100, B20A50, B20GO50, and B20CNT50.

3.2 Performance characteristics

The BTE is the significant parameter in CI engines to evaluate the energy utilization. The inclusion of NPs plays an important role in combustion which enhances the BTE

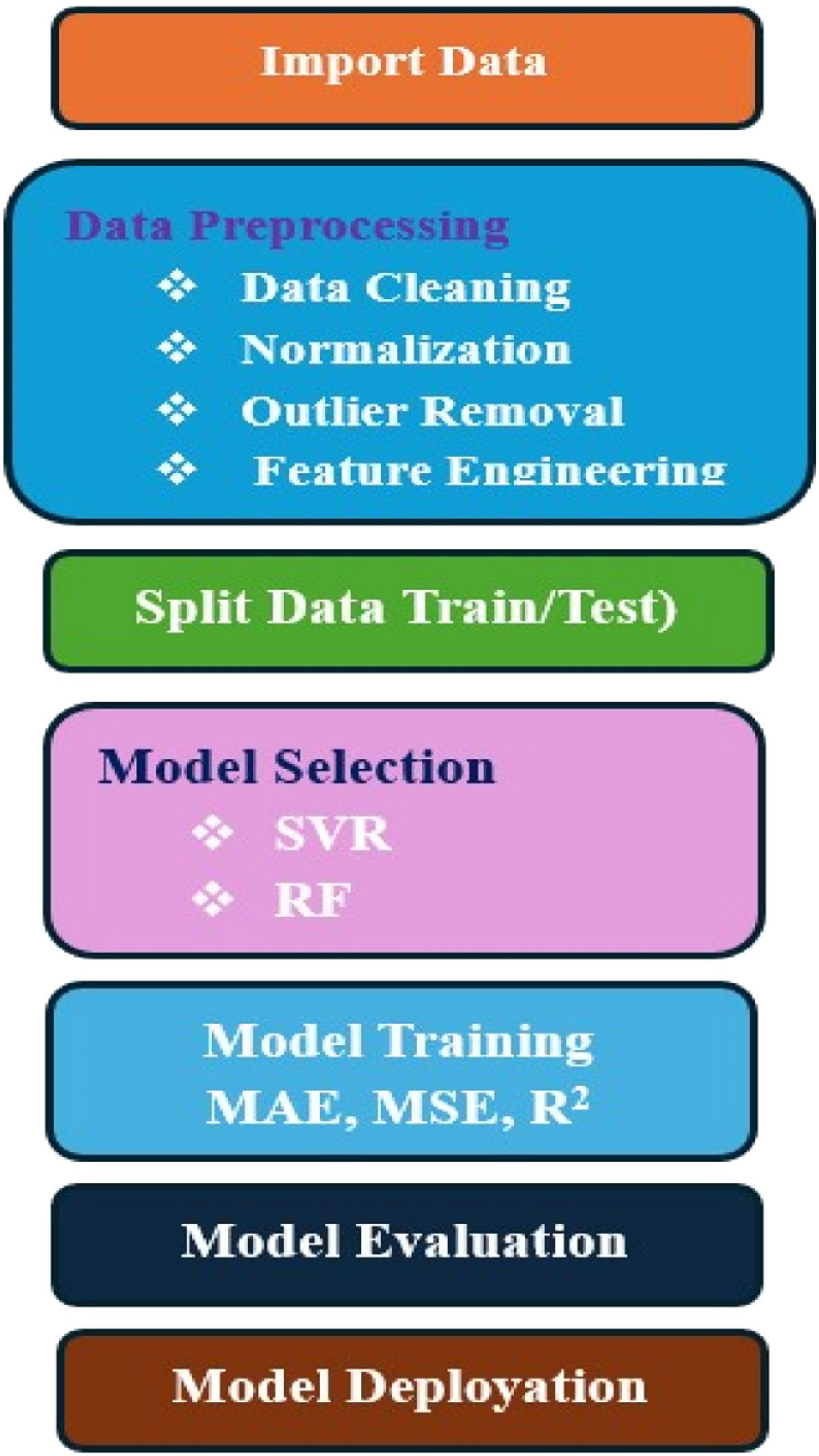

Fig. 5 Regression modeling workflow for engine Performance and Emission variables prediction

Table 5 Simulation governing model and eqs. [30, 37]

Applicable parameters	Equation	Model
Ignition delay period (Tolstov's equation)	$= 3.8\,x\,10^{-6}\,(1-1.60\,x\,10^{-4}\,.\,n)\,\sqrt{\frac{T}{P}}\,.\,e^{\left(\frac{E_a}{8.312T}-\frac{70}{CN+25}\right)}$	Heat Release model
Premixed combustion equation	$\frac{dx}{dt} = \varnothing 0\ (A0\,(mf/Vi).(\sigma_{ud}-x_0).(0.1\sigma_{ud}+x_0)) + \varnothing 1(d\sigma_u/dt)$	
Controlled combustion equation	$\frac{dx}{dt} = \varnothing 1(d\sigma_u/dt) + \varnothing 2\ (A2\,(mf/V).(\sigma_u - x)\,(\varnothing - x))$	
Late combustion equation	$\frac{dx}{dt} = \varnothing_3 A_3 K_t(1-x)\,(\zeta\, b.\varnothing - x)$	
PM formation equation	$[PM] = 565\ X\ (ln\frac{10}{10-BSN})^{1.206}$	Particulate matter emission
NOx emissions	$\frac{dx}{dt} = \varnothing_1(d\sigma_u/dt) + \varnothing_2\ (A_2\,(mf/V_C).(\sigma_u - x)\,(a - x))$	Zeldovich mechanism

and reduces the BSFC. The improvement in performance characteristics is attributed to higher thermal conductivity, large surface to volume ratio, and catalytic activity of NPs which leads to rapid combustion. Figure 7 shows the effect of BTE, and BSFC vs. BP for the prepared fuel blends. It is noticed from the figure that the BTE is found to be improved as the Load is raised. The BTE values observed to be 30.92, 31.76, 32.45, 33.24, and 33.96% for B20, D100, B20A50, B20GO50, and B20CNT50 mixes respectively at higher BP. The maximum BTE values are enhanced by 9.8% for B20CNT50 blend as correlated to B20 sample. Whereas the BSFC values are found to decrease with reference to the BP. The BSFC values are found to be 0.282, 0.321, 0.337, 0.342, 0.347 Kg/kWh for B20CNT50, B20GO50, B20A50, D100, and B20 blends respectively. The highest reduction in BSFC is noticed to be 18.7% for B20CNT50 than the diesel. The performance parameters are found to improve for non-metallic NPs inclusion in B20 sample due to higher thermal conductivity, capability of heat transfer rates, superior rate of reaction due to catalytic activity, and enhanced ignition properties. Further, the improved physio-chemical properties reduce the fuel consumption while, improving power output. In a similar recent study, Çılğın [31] explored to evaluated variation of inclusion of CNTs, and magnesium oxide (MgO) NPs in diesel oil. The results showed that the non-metallic NPs resulted in better performance characteristics when correlated to metal oxide NPs. In another study, Ooi et al. [14] revealed that the inclusion of MWCNTs (at a concentration of 50 mg/l) in palm oil based B20 blend results in improved performance due to improved spray properties, air-fuel interactions, and improved physio-chemical properties.

3.3 Carbon monoxide (CO)

The CO pollutants are affected by quenching, spray patron, and amount of fuel injected. These emissions are majorly emitted by improper ignition of air-fuel mixture. The variation of CO emissions at different loads for tested fuel mixes are depicted in Fig. 8(a). The CO emissions are found to

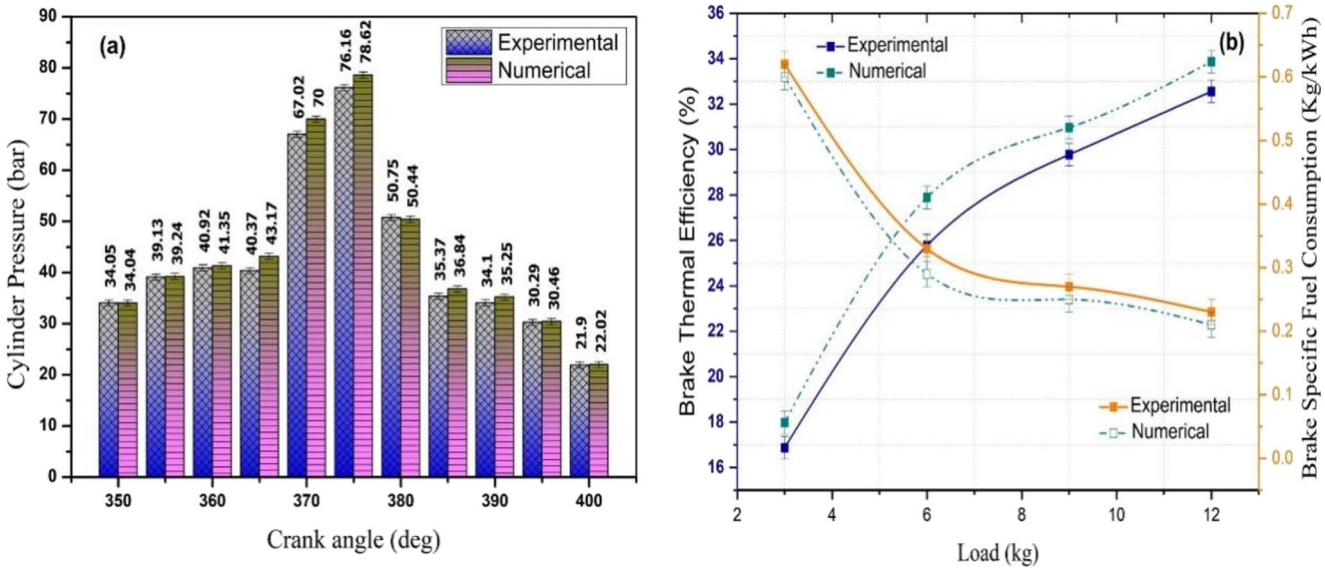

Fig. 6 Illustrates the comparison between experimental and numerically predicted data for (**a**) Cylinder Pressure vs. Crank Angle, and (**b**) BTE and BSFC vs. load based on Diesel R-K simulation software for validation process

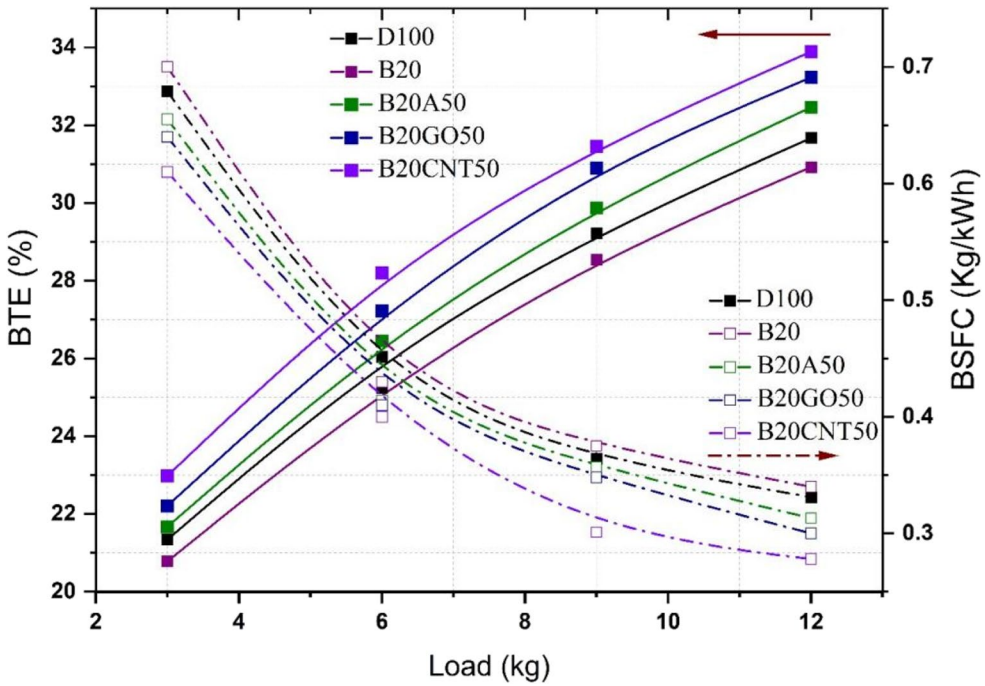

Fig. 7 Shows the effect of BTE, and BSFC vs. Load for prepared blends

be 0.0295, 0.0289, 0.0282, 0.0278, and 0.0272% for D100, B20, B20A50, B20GO50, and B20CNT50 blends at higher BPs respectively. The maximum CO emissions are reduced by 7.79% for B20CNT50 blend due to the oxygen buffer in B20 sample, addition of NPs which enhances combustion properties, facilitates to reduce ID and thereby, decreasing CO emissions. In a similar investigation, Sathish [15] shows that the addition of carbon-based CNT NPs (at a dosage of 50 ppm) reduced CO emissions which is attributed to an increase rate of reaction and leads to comprehensive combustion due to NPs inclusion.

3.4 Carbon dioxide (CO_2)

The CO_2 emissions of various tested fuel blends are shown with respect to the loads in Fig. 8(b). The CO_2 emissions are released due to complete combustion and maximum work output conditions. The CO_2 emissions are found to be 4.26, 4.48, 4.56, 4.64, and 4.74 for D100, B20, B20A50, B20GO50, and B20CNT50 blends at higher BPs respectively. The CO_2 gas is increased by 11.2% for B20CNT50 blend which is due to higher surface to volume ratio, higher thermal conductivity of NPs, Improved heat transfer rate of NPs, reduced ID, and superior combustion. The similar results are observed in an article carried out by Rajpoot et al. [32] that the addition of CNT NPs in biodiesel produced from three generations of feedstocks. The results showed improved CO_2 values (2.53–8.14%) at full load.h.

3.5 Hydrocarbons (HC)

The variation of HC emissions with respect to load for various fuel blends are illustrated in Fig. 8(c). The HC gasses are increased with the load and the HC values are observed to be 9.8, 9.6, 9.4, 9.2, and 8.8 ppm for D100, B20, B20A50, B20GO50, and B20CNT50 blends at higher BPs respectively. The maximum reduction in HC is found by 10.2% for B20CNT50 blend which is ascribed to higher calorific value, improved combustion, shorter ID, short CD. The similar findings are seen in another article explored by Ooi et al. [14] that the addition of CNT NPs in palm oil based B20 sample, results in decreased HC emissions by 16% due to improved physio-chemical properties, proper air-fuel mixing, shorter ID and CD, and superior combustion.

3.6 Nitrogen oxides (NOx)

The higher adiabatic flame temperature during combustion emits NOx pollutants. The NOx emissions are formed at elevated temperature because the nitrogen and oxygen molecules are combined to form NOx emissions. The inclusion of NPs improves the catalytic action, reduces the ID, and it also absorbs the higher temperature produced during combustion. Thereby, the cylinder temperature is decreased and NOx emissions are decreased for nano assisted fuel samples. The effect of NPs on NOx emissions is depicted in Fig. 8(d). The NOx values are found to be 994, 1020, 952, 934, 908 ppm for D100, B20, B20A50, B20GO50, and B20CNT50 blends at higher load respectively. The highest reduction in NOx emission is seen for B20CNT50 mix due to the greater

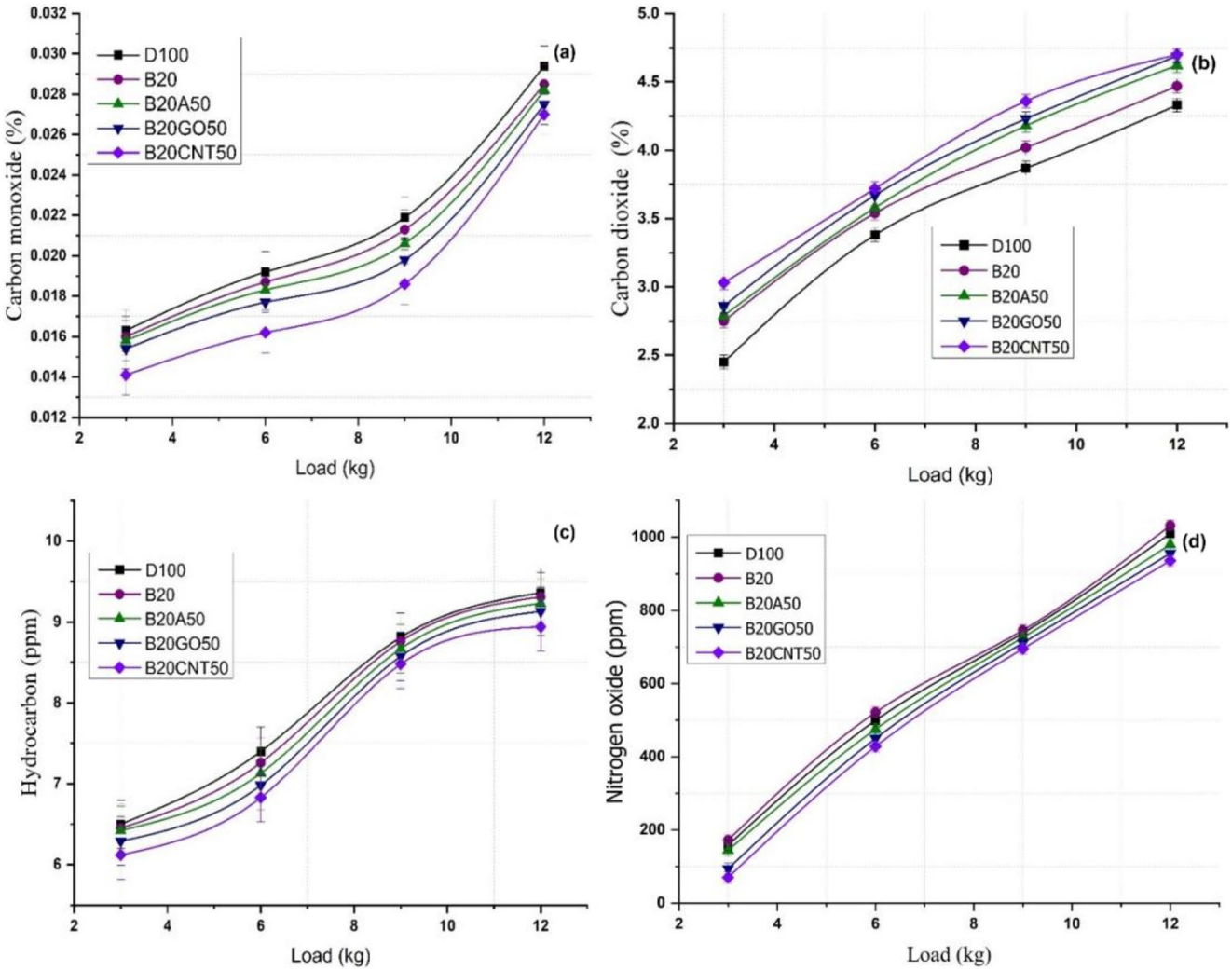

Fig. 8 Presents (**a**) CO vs. Load, (**b**) CO_2 vs. Load, (**c**) HC vs. Load, and (**d**) NOx vs. Load for prepared blends

thermal conductivity of the NPs, and highest heat transfer capacity. In a study carried out by Bikkavolu et al. [5] that the addition of CNT NPs in yellow oleander based B20 mix resulted in reduced NOx emissions due to greater thermal conductivity, and heat capturing property.

3.7 Smoke opacity

The quality of combustion defines the smoke opacity in CI engines. If the complete combustion is achieved, the smoke opacity is minimized and vice versa. The soot concentration/content in the emissions mainly depends on combustion and soot production. The smoke emissions vs. load for various fuels are depicted in Fig. 9. It is observed from the figure that smoke emissions are raised as the load is increased. The smoke values are noticed to be 33.8, 32.79, 32.39, 32.27, and 31.87% for D100, B20, B20A50, B20GO50, and B20CNT50 samples respectively. The maximum decrement in Smoke is found to be 5.71% for B20CNT50 blend as correlated to D100 sample. The reduction in smoke is due to catalytic activity, shortened ID, and improved combustion [5]. In a similar research conducted by Satish [15] that the inclusion of CNTs at a quantity of 50 mg/l in WCO based methyl ester blend decreased smoke due to catalytic effect, and superior combustion.

3.8 Machine learning prediction

Figure 10 presents the R^2values for machine learning model predictions compared to experimental data across key engine performance and emission parameters. High R^2 values, approaching unity, are observed for all outputs BSFC, BTE, CO, CO_2, HC, NO_x, and smoke indicating strong predictive accuracy and excellent correlation between the model predictions and actual measurements. The consistently high R^2 values confirm the models ability

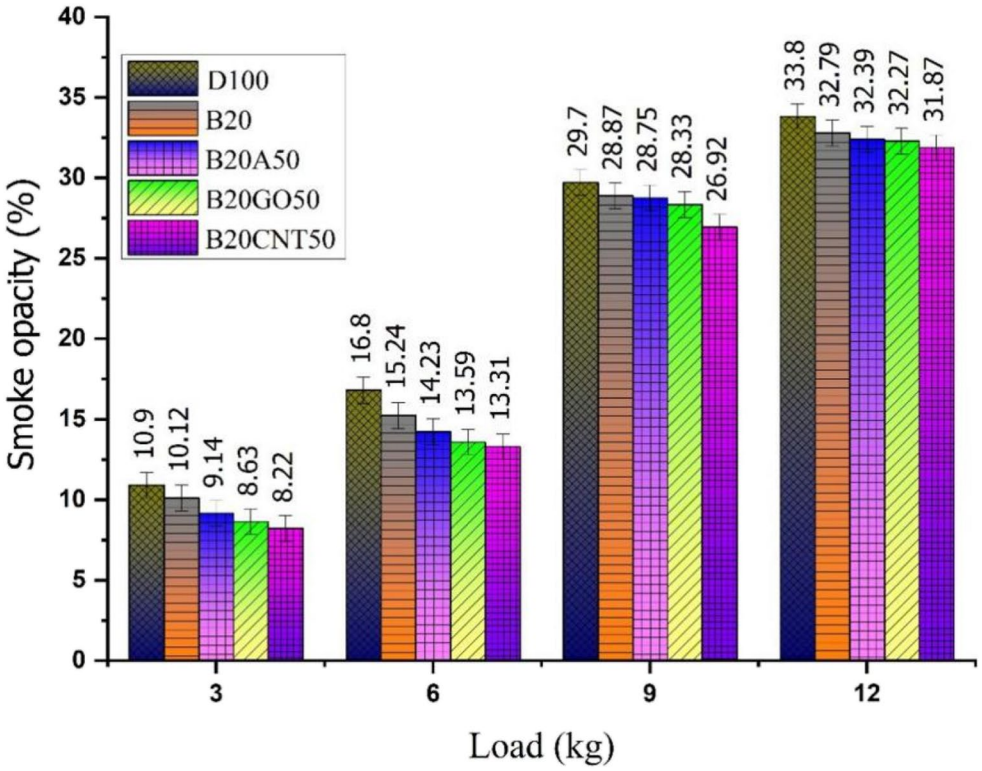

Fig. 9 Illustrates the Smoke opacity vs. Load for the tested fuel blends

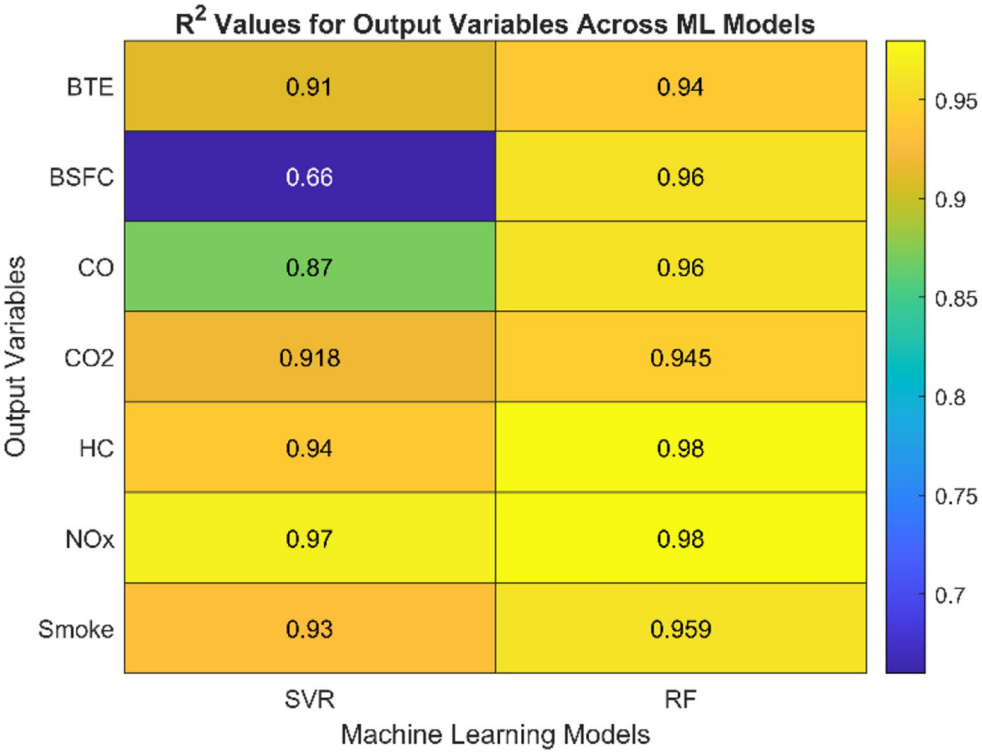

Fig. 10 R^2 values comparing machine learning predictions with experimental data for engine performance and emission parameters

to capture underlying trends and nonlinear behaviors inherent in engine dynamics and combustion-related emissions. This statistical validation further reinforces the reliability and robustness of the developed machine learning models for accurate estimation of engine performance and pollutant outputs. The Table 6 provides a comparative evaluation of the predictive performance of two machine learning models SVR and RF for key engine output features including performance metrics and emission characteristics. The models are assessed using standard statistical performance indicators:

Table 6 Statistical Performance Metrics of SVR and Random Forest Models for Engine Characteristic Predictions

Output features (Engine Characteristics)	ML model	Statistical performance metrics		
		R^2	MAE	MSE
Brake Thermal Efficiency (BTE)	SVR	0.91	1.07	1.46
	RF	0.94	0.83	0.97
Brake Specific Fuel Consumption (BSFC)	SVR	0.66	0.054	0.006
	RF	0.96	0.018	0.0005
Carbon Monoxide Percentage (CO %)	SVR	0.87	0.001	2.93
	RF	0.96	0.0007	9.24
Carbon dioxide (CO_2)	SVR	0.918	0.158	0.038
	RF	0.945	0.132	0.025
Hydrogen carbides (HC)	SVR	0.94	0.213	0.07
	RF	0.98	0.13	0.024
Nitrogen Oxides (NOx)	SVR	0.97	39.99	2634.65
	RF	0.98	28.33	1053.56
Smoke	SVR	0.93	1.88	5.77
	RF	0.959	0.8	0.98

R^2, RMSE, MAE. RF model consistently outperformed SVR among all engine performance and emission characteristics. For BTE, the RF model achieved an R^2 of 0.94, MAE of 0.83%, and MSE of 0.97, demonstrating superior capabilities compared to SVR (R^2 = 0.91, MAE = 1.07%, MSE = 1.46). For BSFC, RF model showed a markedly higher R^2 value of 0.96 with lower MAE (0.018 kg/kWh) and MSE (0.0005) than SVR (R^2 = 0.66, MAE = 0.054 kg/kWh, MSE = 0.006), indicating RF's robustness in capturing nonlinear fuel consumption behavior. In terms of emissions prediction, RF also yielded higher accuracy. For CO emissions, RF achieved an R^2 of 0.96 and an MAE of 0.0007%, outperforming SVR (R^2 = 0.87, MAE = 0.001%). Similarly, for CO_2, the RF model reported R^2 = 0.945, MAE = 0.132%, and MSE = 0.025, compared to SVR's R^2 = 0.918, MAE = 0.158%, and MSE = 0.038. HC predictions were more accurate with RF (R^2 = 0.98, MAE = 0.13 ppm, MSE = 0.024) than SVR (R^2 = 0.94, MAE = 0.213 ppm, MSE = 0.07). For NOx emissions, RF again led with R^2 = 0.98, MAE = 28.33 ppm, and MSE = 1053.56, whereas SVR recorded R^2 = 0.97, MAE = 39.99 ppm, and MSE = 2634.65. Lastly, in predicting Smoke Opacity, RF (R^2 = 0.959, MAE = 0.8%, MSE = 0.98) showed better statistical performance than SVR (R^2 = 0.93, MAE = 1.88%, MSE = 5.77). Overall The results clearly indicate that the Random Forest algorithm exhibits superior generalization ability and predictive precision over SVR, especially for complex and highly variable combustion-related parameters. Thus, RF emerges as a reliable and statistically validated model for predicting engine performance and emission characteristics in dual-fuel engine configurations.

To facilitate clearer interpretation of model performance, comparative bar charts were incorporated, as shown in Fig. 11. These plots present a side-by-side comparison of experimental and ML model predicted values for key engine performance and emission characteristics, including BTE, BSFC, CO, CO_2, HC, NOx, and Smoke Opacity. The SVR and RF models exhibit strong alignment with experimental observations among all parameters and sample indices, confirming their reliability in capturing the nonlinear behavior of dual-fuel combustion systems. The graphical representations provide a visual validation of the numerical performance metrics (R^2, MAE, MSE) reported earlier in Table 6, and serve to enhance interpretability by demonstrating how closely the models replicate actual trends and magnitudes in engine output. The visual agreement shown in Fig. 10 further supports the conclusion that RF offers robust predictive accuracy among both performance and emission variables.

4 Conclusion

The current study explores that the viability of biodiesel-diesel blends with various types of NPs to improve performance, and emission characteristics on a CRDI, CI engine. The investigation used the prepared samples including D100, B20, B20A50, B20GO50, and B20CNT50 samples under varying loads, and the following inferences are given based on the above discussions:

- The biodiesel produced is found to be 97.8%. For better dispersion of NPs in base fuel blend the optimum ratio of NPs to surfactant is optimized at 1:4. The NPs dispersed in karanja oil based B20 blend showed stable, evidenced by the characterization.
- The CP, BTE, and BSFC are compared between experimental and simulation using Diesel R-K simulation software to calibrate the results between experiment and simulation. The CP, and BTE results are found to be 5% variation and BSFC is with in the 10% variation. A very close range of results are noticed between the experimental and simulation. Hence, the prepared blends are further tested on CI engine for overall performance parameters.
- The performance characteristics are observed to be increased (BTE enhanced by 9.8% and BSFC is reduced by 18.7%) for B20CNT50 mix as compared to B20 blend at maximum BP which is due to improved physio-chemical properties, superior thermal conductivity, and greater heat transfer rates of NPs.
- Moreover, the pollutants such as CO, CO_2, HC, and Smoke Opacity are found to be reduced by 7.79, 11.2, 10.2, and 5.71% respectively for B20CNT50 sample when compared to D100 sample at maximum BP. But, the NOx emission is reduced by 10.9% for B20CNT50

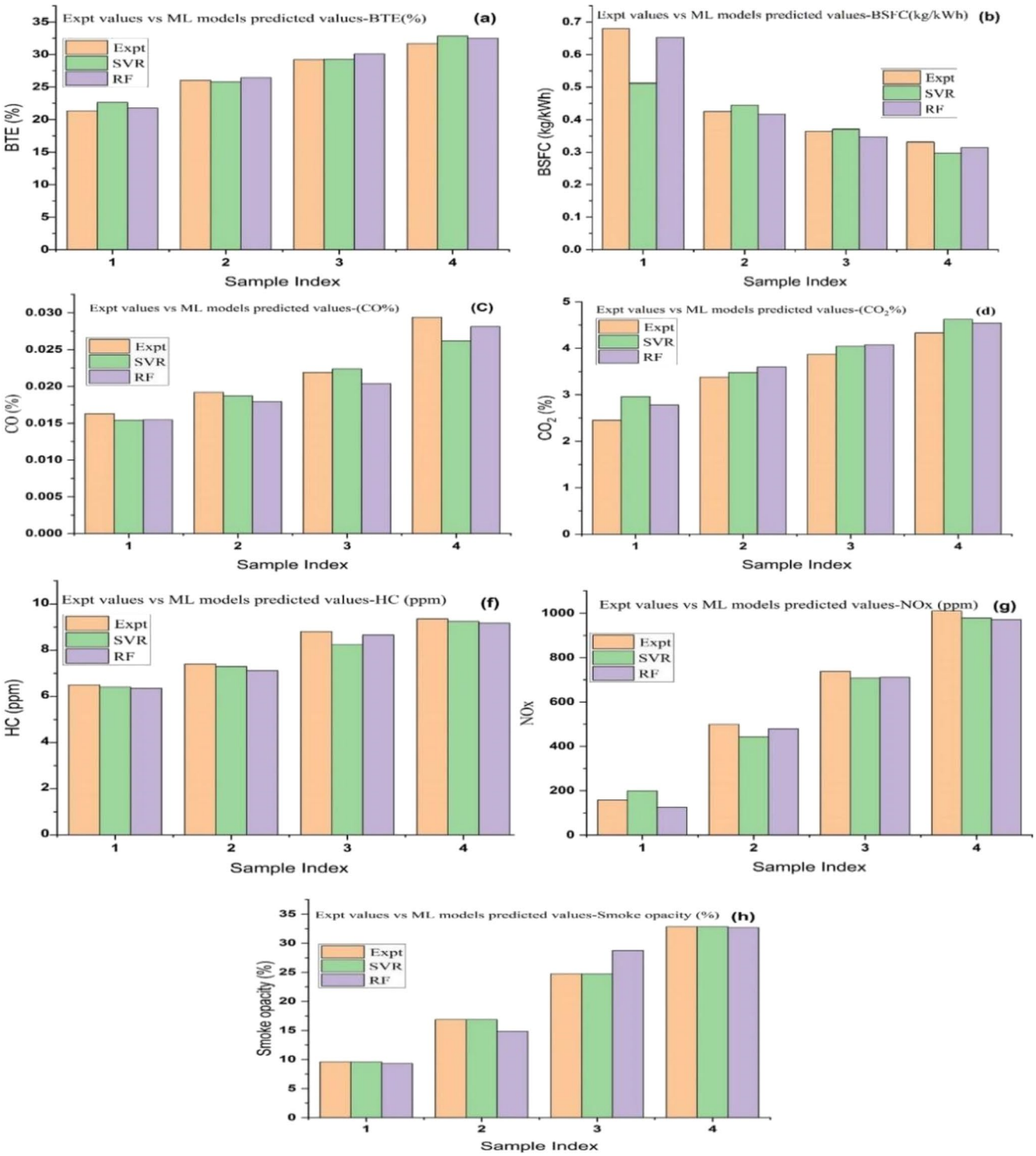

Fig. 11 Validation of Machine Learning Models for Predicting Engine Performance (BSFC, BTE) and Emission Characteristics (CO, CO_2, HC, NO_x, Smoke): Comparison with Experimental Data

mix than the B20 mix at maximum BP. The reduction in emission is due to greater heating value, oxygen content, superior combustion and shorter ID.

- The Random Forest (RF) machine learning method has proven to be an efficient and reliable approach for predicting output variables related to engine performance and emission characteristic curves, offering high accuracy and robustness in handling complex, multidimensional datasets.

Abbreviations

A	Alumina
Al_2O_3	Alluminium Oxide
ANN	Artificial Neural Network
B20	20% of Biodiesel Blended in 80% of Diesel
B20A50	50 mg/L of Aluminium Oxide NPs are dispersed in B20 mix
B20CNT50	50 mg/L of Carbon Nanotube NPs are dispersed in B20 mix
B20GO50	50 mg/L of Graphene NPs are dispersed in B20 mix
BP	Brake Power
BSFC	Brake Specific Fuel Consumption
BTE	Brake Thermal Efficiency
CD	Combustion Duration
CeO2	Cerium dioxide
CI	Compression Ignition
CNTs	Carbon Nanotubes
CO	Carbon monoxide
CO_2	Carbon dioxide
CP	Cylinder Pressure
CRDI	Common Rail Direct Ignition
CuO	Copper Oxide
FESEM	Field Emission Scanning Electron Microscopy
FFA	Free Fatty Acid
FTIR	Fourier Transform Infrared Spectroscopy
GDQ	Graphene Quantum Dot
GNPs	Graphene Nanoplatelets
GO	Graphene Oxide
GPR-FNN	Gaussian Process Regression and Feedback Neural Network
HC	Hydrocarbon
HRR	Heat Release Rate
IC	Internal Combustion
ID	Ignition Delay
KOME	Karanja Oil Methyl Ester
MAE	Mean Absolute Error
MgO	Magnesium oxide
ML	Machine Learning
MSE	Mean Squared Error
MWCNTs	Multi Wall Carbon Nanotubes
NaOH	Sodium Hydroxide
NOx	Nitrogen Oxides
NPs	Nanoparticles
SiO_2	Silicon Oxide
SVR	Support Vector Regression
R^2	Coefficient of Determination
RBF	Radial Basis Function
RF	Random Forest
TiO_2	Titanium Oxide
WHO	World Health Organization
ZnO	Zinc Oxide

Funding This research work is not funded by any funding agency.

Data availability The data is available in the manuscript.

Declarations

Conflict of interest The authors declare that they have no conflict of interest.

References

1. M.U. Haq et al., Influence of nano additives on Diesel-Biodiesel fuel blends in diesel engine: A spray, performance, and emissions study. Energy Convers Manage X **23**, 100574 (2024). https://doi.org/10.1016/j.ecmx.2024.100574
2. G. Pullagura, V.S. Prasad Vanthala, S. Vadapalli, J.R. Bikkavolu, K.R.R. Chebattina, The effect of thermal conductivity and stably dispersed graphene nanoplatelets on *Sterculia foetida* biodiesel–diesel blends for the investigation of performance, emissions, and combustion characteristics on VCR engine. Biofuels **15**(4), 449–460 (2023). https://doi.org/10.1080/17597269.2023.2256105
3. M. Haq et al., Macroscopic spray behavior in pressurized chamber alongside thermal performance of quaternary castor biodiesel with butanol and 1-butoxybutane. Energy **282**, 128912 (2023). https://doi.org/10.1016/j.energy.2023.128912
4. S. Ahmad et al., Performance and emission characteristics of Second-Generation biodiesel with oxygenated additives. Energies **16**(13), 5153–5153 (2023). https://doi.org/10.3390/en16135153
5. J.R. Bikkavolu, S. Vadapalli, K. Rama, G. Pullagura, Effects of stably dispersed carbon nanotube additives in yellow oleander Methyl ester-diesel blend on the performance, combustion, and emission characteristics of a CI engine. Biofuels **15**(1), 67–80 (2023). https://doi.org/10.1080/17597269.2023.2216962
6. Gandhi, Pullagura et al., Performance, combustion and emission reduction characteristics of Metal-based silicon dioxide nanoparticle additives included in ternary fuel (diesel-SMME-iso butanol) on diesel engine. Heliyon. e26519–e26519 (2024). https://doi.org/10.1016/j.heliyon.2024.e26519
7. S. Mathur, H. Waswani, D. Singh, R. Ranjan, Alternative Fuels for Agriculture Sustainability: Carbon Footprint and Economic Feasibility. AgriEngineering. **4**, (4) 993–1015 (2022) https://doi.org/10.3390/agriengineering4040063
8. T. Kalyani, L.S.V. Prasad, A. Kolakoti, Effect of Triacetin as an oxygenated additive in algae biodiesel fuelled CI engine combustion, performance, and exhaust emission analysis. Fuel. **338**, 127366 (2023). https://doi.org/10.1016/j.fuel.2022.127366
9. T. Badawy et al., Selection of second-generation crop for biodiesel extraction and testing its impact with nano additives on diesel engine performance and emissions. Energy **237**, 121605–121605 (2021). https://doi.org/10.1016/j.energy.2021.121605
10. M. Montu, R. Bora, N. Deka, Ahmed, and Dilip Kumar Kakati, Karanja (Millettia pinnata (L) Panigrahi) seed oil as a renewable

raw material for the synthesis of alkyd resin. **61**, 106–114 (2014) https://doi.org/10.1016/j.indcrop.2014.06.048
11. B. Kanimozhi, L. Karthikeyan, T.R. Praveenkumar, S.A. Alharbi, S. Alfarraj, B. Gavurová, Evaluation of Karanja and safflower biodiesel on engine's performance and emission characteristics along with nanoparticles in DI engine. Fuel. **352**, 129101–129101 (2023). https://doi.org/10.1016/j.fuel.2023.129101
12. G. Pullagura, J.R. Bikkavolu, P. V.V.S, R. Prathipati, P.K Seepana, Energy, exergy, and sustainability assessments of a compression ignition diesel engine fueled with Pongamia pinnata oil–diesel blends and nanoparticles. Emergent Mater. (2024). https://doi.org/10.1007/s42247-024-00962-0
13. H.A. Dhahad, A.M. Hasan, M.T. Chaichan, H.A. Kazem, Prognostic of diesel engine emissions and performance based on an intelligent technique for nanoparticle additives. Energy **238**, 121855 (2022). https://doi.org/10.1016/j.energy.2021.121855
14. J.B. Ooi, C.C. Kau, D.N. Manoharan, X. Wang, M.-V. Tran, Y.M. Hung, Effects of multi-walled carbon nanotubes on the combustion, performance, and emission characteristics of a single-cylinder diesel engine fueled with palm-oil biodiesel-diesel blend. Energy **281**, 128350 (2023). https://doi.org/10.1016/j.energy.2023.128350
15. T. Sathish, Combustion and emission performance analyzes on the blend of waste cooking oil / Azadirachta indica oil biodiesel / carbon nano tubes in diesel engines. Int J Thermofluids **24**, 100964 (2024). https://doi.org/10.1016/j.ijft.2024.100964
16. P.K. Nutakki, S.K. Gugulothu, J. Ramachander, Effect of Metal-Based SiO2 nanoparticles blended concentration on performance, combustion and emission characteristics of CRDI diesel engine running on Mahua Methyl ester biodiesel. Silicon Feb. (2021). https://doi.org/10.1007/s12633-021-01001-x
17. S.K. Srinivasan, R. Kuppusamy, P. Krishnan, Effect of nanoparticle-blended biodiesel mixtures on diesel engine performance, emission, and combustion characteristics. Environ Sci Pollut Res **28**, 39210–39226 (2021). https://doi.org/10.1007/s11356-021-13367-x
18. K. Surendrababu, K.G. Muthurajan, M. Prabhahar, S. Prakash, M.S. Kumar, M. Jayakumar, Performance, Emission, and Study of DI Diesel Engine Running on Pumpkin Seed Oil Methyl Ester with the Effect of Copper Oxide Nanoparticles as an Additive. J. Nanomater. **2022** (1) (2022). https://doi.org/10.1155/2022/3800528
19. Prabu, Exploring the impact of aluminum oxide nanoparticles on waste transformer biodiesel blend under variable injection timing. Sustaina. Energy. Res. **11**(1) (2024). https://doi.org/10.1186/s40807-024-00114-2
20. Y. Singh, H.S. Pali, N.K. Singh, A. Sharma, A. Singla, Effect of nanoparticles as additives to the biofuels and their feasibility assessment on the engine performance and emission analysis—A review. Proc Instit Mech Eng Part E J Proc Mech Eng **237**(2), 492–510 (2022). https://doi.org/10.1177/09544089221109723
21. J. Nair, P.P. Kumar, A.K. Thakur, N. Samhita, N. Aravinda, Influence on emissions and performance of CI engine with graphene nanoparticles blended with Karanja biodiesel. AIP Conf Proc. (2021) https://doi.org/10.1063/5.0036142
22. G. Arumugam, K. Muralidharan, Influence of biodegradable graphene oxide nano-platelets blended with Indian Geranium grass biodiesel in a diesel engine. Int J Environ Sci Technol **19**(9), 8613–8632 (2021). https://doi.org/10.1007/s13762-021-03600-y
23. G. Pullagura, P. V.V.S, K.R. Rao Chebattina, Effect of dispersant added graphene nanoplatelets with diesel–Sterculia foetida seed oil biodiesel blends on diesel engine: engine combustion, performance and exhaust emissions. Biofuels **14**(5), 461–472 (2022). https://doi.org/10.1080/17597269.2022.2148876
24. G. Sulochana et al., Impact of multi-walled carbon nanotubes (MWCNTs) on hybrid biodiesel blends for cleaner combustion in CI engines. Energy **303**, 131911–131911 (2024). https://doi.org/10.1016/j.energy.2024.131911
25. G. Soundararajan et al. Synergistic effects of graphene quantum Dot additives in waste plastic oil blends: combustion stability and emission reductions analysis. Results Eng. 104130–104130 (2025). https://doi.org/10.1016/j.rineng.2025.104130
26. V.K. Varma, A. Sharma, S. Singh, Application of artificial neural networks for performance and emission prediction of biodiesel-fueled CRDI engines. Fuel. **288**, 119701 (2021)
27. Y. Liao, H. Zhang, B. Xu, Optimization of injection parameters in biodiesel-fueled CRDI engines using support vector machine learning. Energy. Conv. Manag. **277**, 116544 (2023)
28. A.M. Yusuf, S. Kumar, R. Singh, Influence of cerium oxide nanoparticles on the combustion and emission characteristics of biodiesel blends in diesel engines. Renew. Energy. **190**, 145–154 (2022)
29. N. Amrulloh, M.M. Rahman, S.A. Sulaiman, Evaluation of ZnO nanoparticles in biodiesel blends on engine performance and emission behavior. J. Clean. Prod. **424**, 139582 (2024)
30. M.F. Al-Dawody, A.A. Jazie, H. Abdulkadhim Abbas, Experimental and simulation study for the effect of waste cooking oil Methyl ester blended with diesel fuel on the performance and emissions of diesel engine. Alexandria Eng J **58**(1), 9–17 (2019). https://doi.org/10.1016/j.aej.2018.05.009
31. Erdal, Çılğın, Synergistic effects of SWCNT and MgO nanoparticle additives on engine performance and emissions: a laboratory analysis approach. Biofuels. 1–21 (2025). https://doi.org/10.1080/17597269.2025.2460135
32. S. Rajpoot, G. Saini, H.M. Chelladurai, A.K. Shukla, T. Choudhary, Comparative combustion, emission, and performance analysis of a diesel engine using carbon nanotube (CNT) blended with three different generations of biodiesel. Environ Sci Pollut Res **30**(60), 125328–125346 (2023). https://doi.org/10.1007/s11356-023-28965-0
33. A. Cao, C. Xu, J. Liang, D. Wu, B. Wei, X-ray diffraction characterization on the alignment degree of carbon nanotubes. Chem. Phys. Lett. **344**(1–2), 13–17 (2001)
34. S. Wang, X. Li, S. Wang, Y. Li, Y. Zhai, Synthesis of γ-alumina via precipitation in ethanol. Mater. Lett. **62**(20), 3552–3554 (2008)
35. J. E et al., Experimental investigation on performance and economy characteristics of a diesel engine with variable nozzle turbocharger and its application in urban bus. Energy. Conv. Manag. **193**, 149–161 (2019) https://doi.org/10.1016/j.enconman.2019.04.062
36. K.N. Balan, U. Yashvanth, P. Booma Devi, T. Arvind, H. Nelson, Y. Devarajan, Nov., Investigation on emission characteristics of alcohol biodiesel blended diesel engine, **41**(15) 1879–1889 (2018) https://doi.org/10.1080/15567036.2018.1549166
37. A.S. Rajpoot, T. Choudhary, H. Chelladurai, T.N. Verma, A. Pugazhendhi, Sustainability analysis of spirulina biodiesel and their blends on a diesel engine with energy, exergy and emission (3E's) parameters. Fuel. **349**, 128637–128637 (2023). https://doi.org/10.1016/j.fuel.2023.128637